Dynamic stabilization of the two-stream instability during longitudinal compression of intense charged particle beam propagation through background plasma

Edward A. Startsev* and Ronald C. Davidson
Plasma Physics Laboratory, Princeton University, Princeton, New Jersey 08543

The electrostatic two-stream instability for a cold, longitudinally-compressing intense ion beam propagating through a background plasma has been investigated both analytically and numerically. The linear development of the instability and its saturation are examined from the point of view of wave dynamics, where the plasma waves are represented as quasi-particles characterized by their position $x(t)$, wavenumber $k(t)$ and energy (or frequency) $\omega(t)$. It is found that the longitudinal beam compression strongly modifies the space-time development of the instability. In particular, the dynamic compression leads to a significant reduction in the growth rate of the two-stream instability compared to the case without an initial velocity tilt.

PACS: 52.35.Qz; 52.59.S9; 52.58.Hm

Keywords: Two-stream instability; Dynamic stabilization; Charged-particle beams

1. Introduction

To achieve the high focal spot intensities necessary for high energy density physics and heavy ion fusion applications, the ion beam pulse must be compressed longitudinally by factors of one hundred or more before it is focused onto the target. The longitudinal compression is achieved by imposing an initial velocity profile tilt on the drifting beam in vacuum [1–3, 6]. To achieve maximum longitudinal compression, the space charge of the beam is neutralized by propagation of the beam pulse through a dense neutralizing background plasma [2–7]. If the space charge is fully neutralized by the plasma, the final compression is limited only by the initial longitudinal temperature of the beam ions and possible collective processes (such as the two-stream instability [2, 8–11]) which may prevent full neutralization of the beam space charge. The beam's longitudinal thermal spread which can stabilize the instability also inhibits full longitudinal compression. In a recent paper, we made use of macroscopic fluid model [2, 12] to investigate both analytically and numerically the electrostatic two-stream instability for a cold, longitudinally-compressing charged particle beam propagating through a background plasma. It was found that the longitudinal beam compression strongly modifies the space-time development of the two-stream instability. In particular, it is found that the dynamic compression leads to a significant reduction in the growth rate of the two-stream instability compared to the case without an initial velocity tilt.

The analysis presented here employs a geometrical optics approach to the wave dynamics. This type of analysis has been used to study the effects of possible density gradients on the two stream-instability [13]. In the case considered here, the instability growth is limited by the velocity tilt. Indeed, for small beam density, the instability between beam ions and the background plasma electrons requires that the resonance condition $\omega \simeq kV_b \simeq \omega_{pe}$ be satisfied for continuous growth. Here, ω_{pe} is the electron plasma frequency associated with the plasma electrons, k is the axial wavenumber of the perturbation , and V_b is the beam velocity. As shown in Sec. 4, the perturbation frequency changes with time due to the time-dependent beam velocity and beam density profile, and the mode eventually detunes out of resonance and the instability ceases. The present analysis takes into account the effects of the velocity tilt and allows the level of saturation to be determined. Numerical simulations using the particle-in-cell code LSP have recently appeared in the literature that address the practical requirements for neutralized propagation of heavy ion beams for cases with and without longitudinal compression [4–6]. Some preliminary numerical simulations of the possible effects of longitudinal compression on the two-stream instability for longitudinally-compressing heavy-ion beams have also been reported [6]. This paper is organized as follows. In Sec. 2, we consider the unperturbed propagation of the ion beam in the background plasma. In Sec. 3 we describe the quasi-particles model which is used to analyze the instability, where the plasma waves are represented as quasi-particles characterized by their position $x(t)$, wavenumber $k(t)$ and energy (or frequency) $\omega(t)$. In Sec. 4, we apply this model to analyze the two-stream instability between the beam ions and background plasma electrons, and in Sec. 5 we use the quasi-particle model to analyze the two-stream instability between the neutralizing plasma electrons and the plasma ions. Finally, the results are summarized in Sec. 6.

2. Unperturbed propagation

It is assumed that a semi-infinite ion beam with a

*Corresponding author
E-mail address: estarts@pppl.gov (E.A.Startsev)

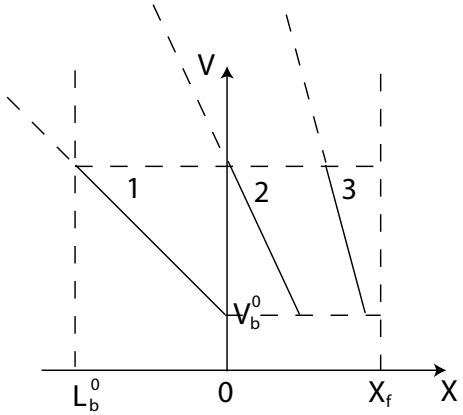

FIG. 1: Plot of the ion beam phase space at different times during the compression. Line 1 corresponds to $t = 0$.

sharp leading edge enters the region containing background plasma at time $t = 0$ and $x = 0$ with velocity V_b^0 and density n_b^0. The beam is uniformly compressing in the longitudinal direction as it propagates inside the chamber and reaches the maximum compression at time $t = T_f$ at the point $x = X_f = T_f V_b^0$ away from the beam entry point $x = 0$ into the chamber. The unperturbed beam propagation is illustrated in Fig. 1, where the beam phase space is plotted at different times during the compression. The transition from the solid to dashed lines in Fig. 1 identifies the end of the real beam pulse with finite initial length L_b^0. The frequently used parameter, the longitudinal "velocity tilt" $\Delta V_b^0/V_b^0$, is related to the compression distance X_f and the initial beam pulse length L_b^0 by

$$\Delta V_b^0/V_b^0 = L_b^0/X_f. \tag{1}$$

It is also assumed that the ion beam propagation in the background plasma is both charge neutralized and current neutralized, where the quasi-neutrality conditions are given by

$$\bar{n}_e = Z_b \bar{n}_b + n_0, \tag{2}$$

$$\bar{n}_e \bar{V}_e = Z_b \bar{n}_b \bar{V}_b. \tag{3}$$

Here, $\bar{n}_j$ and $\bar{V}_j$ denote the dynamically changing unperturbed density and flow velocity of the beam ions (j=b) and background plasma electrons (j=e), and $n_0 = const.$ (independent of x and t) is the uniform density of the background plasma ions (assumed singly-ionized). In Eqs. (2) and (3), Z_b is the charge state of the beam ions. The quasi-neutrality condition is slightly violated due to the finite electron mass in the force balance equation for the plasma electrons [2]

$$e\bar{E} = -m_e \left(\frac{\partial \bar{V}_e}{\partial t} + \bar{V}_e \frac{\partial \bar{V}_e}{\partial x} \right). \tag{4}$$

The zero-order solution for the beam density and velocity are given by [2]

$$\bar{n}_b(t) = \frac{n_b^0 T_f}{T_f - t}, \tag{5}$$

$$\bar{V}_b(t,x) = \frac{V_b^0 T_f - x}{T_f - t}. \tag{6}$$

Substituting Eqs. (2), (3) and (6) into Eq. (4), we obtain for the unneutralized electric field

$$e\bar{E} = -2m_e \frac{Z_b n_b^0}{n_0} \frac{(X_f - x)}{[(1 - t/T_f) + (Z_b n_b^0/n_0)]^2 T_f (T_f - t)}. \tag{7}$$

Using Poisson's equation $\partial \bar{E}/\partial x = 4\pi e \delta\bar{n} = 4\pi e(Z_b \delta\bar{n}_b - \delta\bar{n}_e)$, we obtain for the unneutralized charge density

$$\frac{\delta\bar{n}(x,t)}{Z_b \bar{n}_b(t)} = \frac{2}{\omega_{pe}^2 T_f^2} \frac{1}{\left[\left(1 - \frac{t}{T_f}\right) + \frac{Z_b n_b^0}{n_0}\right]^2}, \tag{8}$$

where $\omega_{pe}^2 \equiv 4\pi n_0 e^2/m_e$ is the plasma frequency-squared of the background plasma electrons. In what follows we make use of the parameter

$$\epsilon \equiv 1/(\omega_{pe} T_f) \ll 1. \tag{9}$$

It will be shown that the resonant two-stream instability develops and saturates everywhere in the background plasma region except close to the compression point $x = X_f$ during the time interval when $1 - t/T_f \sim 1$. It follows from Eq. (8) that $\delta\bar{n}(x,t)/Z_b \bar{n}_b(t) \simeq 2\epsilon^2$ during this time interval, and therefore for perturbations with amplitude $|\delta\tilde{n}(x,t)|/Z_b \bar{n}_b(t) \gg \epsilon^2$, the beam can be considered as fully neutralized by the background plasma.

In what follows, we consider the case of a semi-infinite beam (see Fig. 1). For a beam with finite initial length L_b^0, the trailing beam end will trace the trajectory $x_{end}(t) = V_b^0 t(1 + L_b^0/X_f) - L_b^0$. In this case, the present analysis is applicable everywhere between the leading and trailing edges of the beam, $max\{0, x_{end}(t)\} \leq x \leq x_{head}(t) = V_b^0 t$, where the beam can drive the background plasma unstable. Behind the beam, for $0 \leq x < x_{end}(t)$, the plasma will be left with remnant collective oscillations with constant amplitude, which are excited by the propagating beam.

The full neutralization assumptions in Eqs. (2) and (3) are also violated at the beam head, where the time-changing magnetic field induces a longitudinal electric field which acts on the plasma electrons to cause a flow of return current opposite to the injected current. The distance from the beam head, where the current and charge neutrality conditions are violated, depends on the smoothness of the beam head density profile [7]. Generally, if the density profile of the beam increases from zero to it's maximum value over a distance larger than V_{b0}/ω_{pe}, then the the beam charge is fully neutralized. In addition, the beam current will be neutralized if the

beam diameter is much larger than the collisionless skin-depth c/ω_{pe}.

In what follows, we considered the case of a low-density ion beam propagating through a background plasma with $\bar{\delta} \equiv Z_b n_b^0/n_0 \ll 1$. In this case, one can identify two separate stages (the fast and the slow stages) of the two-stream instability. During the fast stage, the instability is between the neutralizing plasma electrons, flowing with the velocity $\sim (n_b/n_e)V_b$, and the background plasma ions. During this initial stage, the beam ions are relatively unaffected. We consider this stage of the instability in Sec. 5. At later times, a two-stream instability between the beam ions and the neutralizing background electrons may develop. This later stage of instability, which directly affects the beam particles, is analyzed in Sec. 4.

3. Space-time dynamical description of the instability

In what follows we examine the development of the instability and its saturation from the point of view of wave dynamics [2] where the plasma waves are represented as quasi-particles characterized by their position $x(t)$, wave-number $k(t)$ and energy (or frequency) $\omega(t)$. The quasi-particle dynamics are described by the equations of motion

$$\frac{dx}{dt} = \frac{\partial\omega}{\partial k} = -\frac{\partial D/\partial k}{\partial D/\partial w}, \tag{10}$$

$$\frac{dk}{dt} = -\frac{\partial\omega}{\partial x} = \frac{\partial D/\partial x}{\partial D/\partial w}, \tag{11}$$

$$\frac{d\omega}{dt} = \frac{\partial\omega}{\partial t} = -\frac{\partial D/\partial t}{\partial D/\partial w}, \tag{12}$$

and the quasi-particle dynamics takes place on the surface $D = 0$. Here D is the linear dispersion function.

4. Instability between the beam ions and plasma electrons

In this section we consider the instability between the beam ions and the neutralizing plasma electrons. In this case, the dispersion function D is defined by

$$D = 1 - \frac{\omega_{pe}^2}{\omega^2} - \frac{\omega_{pb}^2(t)}{[\omega - kV_b(x,t)]^2}, \tag{13}$$

and the quasi-particle dynamics takes place on the surface $D = 0$. Substituting Eq. (13) into Eqs. (10)–(12), we obtain the closed system of equations for $x(t)$ and $p(t) = k(t)V_b(x,t)/\omega(t)$ given by

$$\frac{dx}{dt} = \frac{V_b(x,t)}{1+(1-p)^3/\delta(t)}, \tag{14}$$

$$\frac{dp}{dt} = \left[p - \frac{p^2}{1+(1-p)^3/\delta(t)}\right]\frac{1}{V_b(x,t)}\frac{\partial V_b(x,t)}{\partial t} - \left[\frac{p(1-p)/2}{1+(1-p)^3/\delta(t)}\right]\frac{1}{\delta(t)}\frac{\partial\delta(t)}{\partial t}. \tag{15}$$

Here $\delta(t) = \omega_{pb}^2(t)/\omega_{pe}^2$, and

$$\frac{\omega}{\omega_{pe}} = \left[1 + \frac{1}{(1-p)^2/\delta(t)}\right]^{1/2}. \tag{16}$$

It follows from Eq. (16) that for $\delta \ll 1$ the maximum growth rate occurs for $p \sim 1$, which corresponds to perfect resonance. Equation (15) describes the detuning from resonance for the particular quasi-particle under consideration. For a uniform non-compressing ion beam with $V_b = const.$, Eqs. (14) and (15) are easily solved to give

$$p = p_0, \tag{17}$$

$$x - \frac{V_b t}{1+(1-p)^3/\delta} = x_0, \tag{18}$$

with general solution for $p(x,t)$ given by

$$x - \frac{V_b t}{1+(1-p)^3/\delta} = f(p). \tag{19}$$

We are interested in obtaining self-similar solutions which correspond to asymptotic solutions independent of the initial conditions. Such a solution is given by

$$(1-p)^3 = \delta\left[\frac{V_b t - x}{x}\right]. \tag{20}$$

For $\delta^{1/3}[x/(V_b t - x)]^{2/3} \ll 1$, we obtain from Eq. (16)

$$\frac{\omega}{\omega_{pe}} = 1 + \frac{(i\sqrt{3}-1)}{2}\frac{\delta^{1/3}}{2}\left[\frac{x}{V_b t - x}\right]^{2/3}, \tag{21}$$

where only the unstable solution with positive imaginary part of the frequency is retained. From Eq. (21), we obtain the gain function

$$G(x,t) = \int_{x/V_b}^{t} Im\omega(x,\bar{t})d\bar{t} = \frac{3\sqrt{3}}{4}\frac{\omega_{pe}}{V_b}\delta^{1/3}x^{2/3}(V_b t - x)^{1/3}. \tag{22}$$

The gain function in Eq. (22) coincides with the gain function obtained by direct solution of the linearized fluid equations [8]. If follows from Eq. (22) that the gain function never saturates. This is because the quasi-particle's detuning factor $p - 1$ does not change with time [see Eq. (17)], and quasi-particles which were initially in resonance will stay in resonance indefinitely.

For the case where the beam velocity $V_b(x,t)$ changes dynamically according to Eq. (6), it follows that Eqs. (14) and (15) cab be expressed as

$$\frac{dp}{dT} = p - \frac{p(1+p)/2}{1+(1-p)^3/\delta}, \tag{23}$$

$$\frac{dY}{dT} = \frac{1}{1+(1-p)^3/\delta}, \tag{24}$$

where $Y = \log[1/(1 - x/X_f)]$ and $T = \log[1/(1 - t/T_f)]$. Introducing the quantity q defined by $p = 1 + q\delta^{1/3}$ in Eq. (15), we obtain equations for q valid to leading order in the small parameter δ, i.e.,

$$\delta^{1/3}\left(\frac{dq}{dT} + \frac{5}{6}q\right) = -q^3, \quad (25)$$

$$\frac{d\xi}{dT} = -q^3, \quad (26)$$

$$\frac{\omega}{\omega_{pe}} = \hat{\omega} = \left[1 + \frac{\delta^{1/3}}{q^2}\right]^{1/2}, \quad (27)$$

where $\xi = T - Y$. As shown below, the instability in this case saturates when $q \sim \delta^{1/6} \ll 1$, which justifies retaining only leading-order terms in Eqs. (25) and (26). The solution to Eqs. (25) and (26) is given by

$$\exp(-2T)\left[\frac{\delta^{1/3}(T)}{q^2} + 1\right] = I \quad (28)$$

$$\xi = \xi_0 - \delta(T)^{1/2}\int_0^T d\bar{T}\frac{\exp[(\bar{T} - T)/2]}{\left[I\exp(2\bar{T}) - 1)\right]^{3/2}}, \quad (29)$$

where I and ξ_0 are invariants of the motion. Making use of Eqs. (27), (28) and (29), we obtain the asymptotic solution for $\hat{\omega}(\xi, T) = \omega/\omega_{pe}$, which is independent of the initial conditions, i.e.,

$$\xi = -2\delta(T)^{1/2}\int_{\exp(-T/2)}^1 \frac{d\eta}{\left[\eta^4\hat{\omega}^2 - 1)\right]^{3/2}}. \quad (30)$$

The corresponding gain function $G(x, t)$ is given by

$$G(x,t) = \int_{x/V_b^0}^t Im\omega(x,\bar{t})d\bar{t} =$$
$$= \omega_{pe}T_f\exp(-Y)Im\int_0^\xi d\bar{\xi}\exp(-\bar{\xi})\hat{\omega}(\bar{\xi}, Y). \quad (31)$$

It can be shown from Eq. (30) that $Im\hat{\omega} \sim (\delta)^{3/2}/\xi^3$ for $\xi/\delta^{1/2} \gg 1$ so that we can neglect the exponential contribution in Eq. (31) to the integral, and also extend the upper integration limit to infinity for $\xi \gg \delta^{1/2}$. In addition, we can also replace $T \to Y$ on the right-hand side of Eq. (30). Integrating Eq. (31) by parts, and taking into account that $Im[\hat{\omega}(\xi)]\xi \sim 1/\xi^2 \to 0$ for $\xi \to \infty$, and $Im[\hat{\omega}(\xi)]\xi \sim \xi^{2/3} \to 0$ for $\xi \to 0$, we obtain

$$G = \omega_{pe}T_f\exp(-Y)Im\int_0^\infty d\xi\hat{\omega}(\xi, Y) = \quad (32)$$
$$-\omega_{pe}T_f\exp(-Y)Im\int_{\hat{\omega}(0,Y)}^{\hat{\omega}(\infty,Y)} d\hat{\omega}\xi(\hat{\omega}, Y)$$
$$= -2\alpha\sqrt{1 - X}Im\int_{\sqrt{1-X}}^1 \frac{d\eta}{\sqrt{\eta^4 - 1/\hat{\omega}^2}}\Bigg|_{\hat{\omega}(0,Y)}^{\hat{\omega}(\infty,Y)},$$

where $\alpha = \delta_0^{1/2}\omega_{pe}T_f = \omega_{pb}^0 T_f$. Equation (30) has several solutions. The solution with positive imaginary part to the frequency, which corresponds to instability, corresponds to $\hat{\omega}^2(\infty, Y) = 1$ and $\hat{\omega}^2(0, Y) = \infty$. Therefore, using Eq. (32), we obtain

$$G(X) = 2\alpha\sqrt{1 - X}\int_{\sqrt{1-X}}^1 \frac{d\eta}{\sqrt{1 - \eta^4}}$$
$$= \alpha\sqrt{2(1 - X)}F[\arccos(\sqrt{1 - X})|1/2], \quad (33)$$

where $X = x/X_f$ and $F(x|\alpha) \equiv \int_0^x d\theta/\sqrt{1 - \alpha\sin^2\theta}$ is an elliptic integral of the first kind. The gain function in Eqs. (33) is identical to the gain function obtained by finding the asymptotic solution of the linearized fluid equations [2]. The region where it is valid, $\xi \gg \delta^{1/2}$ or $\tau = \omega_{pe}(t - x/V_b) \gg \alpha\sqrt{1 - x/X_f}$, also coincides with region where the asymptotic solution is valid [2]. The fact that we have obtained identical expressions for the gain function, demonstrates the consistency of the approximations used in the derivations. The method of quasi-particles also clarifies the dynamics of the instability in a physically intuitive way. Figure 2 shows the normalized instability gain function $G(x, t)/\alpha$ plotted as a function of distance x/X_f at different times $t/T_f = 0.15$ (1), 0.25 (2), 0.35 (3), 0.45 (4), 0.55 (5), 0.65 (6), and 0.75 (7) obtained numerically by solving Eqs. (14)–(16) (solid curves) and compared with the analytical result in Eq. (33) (dashed curve). Figure 3 shows a comparison of the gain function in Eq. (33) with the gain function for a beam with zero velocity tilt [Eq. (22)] at $t = T_f$ for $\delta_0 = (\omega_{pb}^0/\omega_{pe})^2 = 10^{-3}$ and $\alpha^2 = (\omega_{pb}^0 T_f)^2 = 1000.$, i.e.,

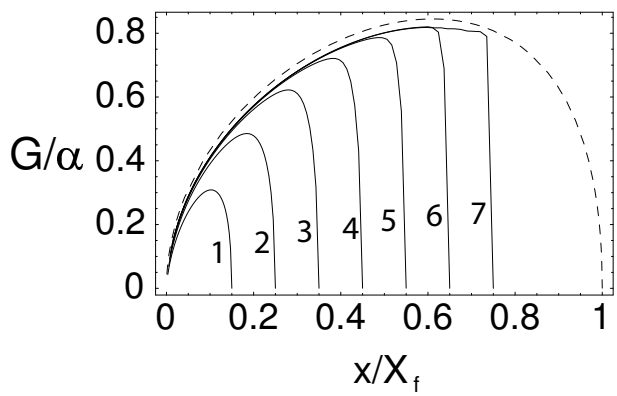

FIG. 2: The normalized instability gain function $G(x, t)/\alpha$ is plotted as a function of distance x/X_f at different times $t/T_f = 0.15$ (1), 0.25 (2), 0.35 (3), 0.45 (4), 0.55 (5), 0.65 (6), and 0.75 (7) obtained numerically (solid curve) and compared with the analytical result in Eq. (33) (dashed curve).

$$G_{notilt}(X, t = T_f) = \alpha\frac{3\sqrt{3}}{4}\frac{X^{2/3}(1 - X)^{1/3}}{\delta_0^{1/6}}. \quad (34)$$

As evident from Fig. 3, for $\delta^{1/6} \ll 1$ the velocity tilt

significantly reduces the growth rate compared to the case of a beam with zero initial velocity tilt.

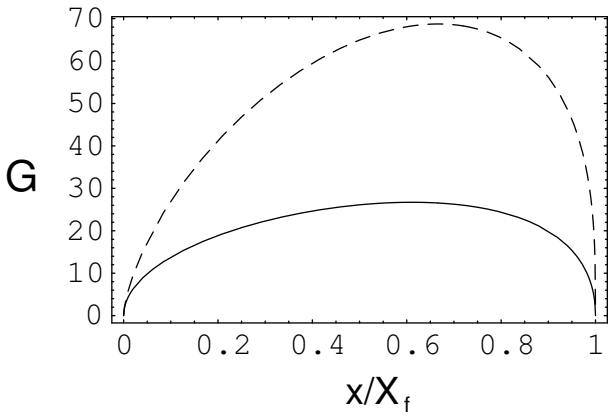

FIG. 3: Comparison of the instability gain as a function of x/X_f for a beam with velocity tilt (solid curve) and without velocity tilt (dashed curve) for $\delta_0 = (\omega_{pb}^0/\omega_{pe})^2 = 10^{-3}$ and $\alpha^2 = (\omega_{pb}^0 T_f)^2 = 1000$.

5. Instability between the plasma ions and the neutralizing plasma electrons

In this section we consider the two-stream instability due to the flow of the neutralizing plasma electrons though the background plasma ions. In this case, the dispersion function D is defined by

$$D = 1 - \frac{\omega_{pi}^2}{\omega^2} - \frac{\omega_{pe}^2(t)}{[\omega - kV_e(x,t)]^2}. \tag{35}$$

Here,

$$\omega_{pe}^2(t) = \omega_{pe}^2(t=0)\left[1 + \bar{\delta}(t)\right], \tag{36}$$

$$V_e(x,t) = \bar{\delta}(t) V_b(x,t), \tag{37}$$

are the background electron plasma frequency-squared and the electron flow velocity, respectively. In Eqs. (36) and (37), $\bar{\delta}(t) = Z_b \bar{n}_b(t)/n_0 \ll 1$. Substituting Eqs. (36) and (37) into Eqs. (10)–(35), we obtain the closed system of equations for $Y(T)$ and $p(T) = (kV_e - \omega)/\omega_{pe}$ given by

$$\frac{dY}{dT} = \frac{\bar{\delta}(T)}{1 - m^{1/2}[p^2-1]^{3/2}}, \tag{38}$$

$$\frac{dp}{dT} = 2p\left[\frac{1 + m^{-1/2}[p^2-1]^{-1/2}}{1 - m^{-1/2}[p^2-1]^{-3/2}}\right], \tag{39}$$

where

$$\frac{\omega}{\omega_{pi}} = \frac{p}{[p^2-1]^{1/2}}, \tag{40}$$

which follows from $D = 0$. Here, we have made use of Eqs. (36) and (37) together with Eqs. (5) and (6), and introduced the new variables $Y = \log[1/(1 - x/X_f)]$, $T = \log[1/(1 - t/T_f)]$, and $\hat{\omega} = \omega/\omega_{pi}$. In Eqs. (39) and (40), the parameter m is defined as $m \equiv m_i/m_e \gg 1$, and $\bar{\delta}(T) = \bar{\delta}_0 \exp(T) \ll 1$.

It follows from Eqs. (38)–(40) that for $m \gg 1$ the perturbations propagate only for $p - 1 \lesssim 1/m^{1/3}$, which corresponds to a resonance in Eq. (35). If this condition is not satisfied, the perturbations are unstable but they do not propagate. Since the perturbations are introduced by the beam at the beam entrance into the plasma, these perturbations will not propagate into the plasma, and therefore will not contribute to the dynamics of the instability anywhere inside the plasma. Near the resonance, Eqs. (38)-(40) can be rewritten as

$$\frac{d\hat{\omega}}{dT} = -\frac{2\hat{\omega}^3}{1 - \hat{\omega}^3/m^{1/2}}, \tag{41}$$

$$\frac{dY}{dT} = -\frac{\bar{\delta}(T)}{m^{1/2}} \frac{\hat{\omega}^3}{1 - \hat{\omega}^3/m^{1/2}}. \tag{42}$$

The validity condition $p - 1 \lesssim m^{-1/3}$ corresponds to $m^{1/6} \lesssim \hat{\omega}$. Equations (41) and (42) can be easily solved if we neglect the time dependence of $\bar{\delta}(T) = \bar{\delta}_0 \exp(T)$. As shown later, this assumption is justified for sufficiently small velocity tilt. With this approximation in mind, the solution to Eqs. (41) and (42) is given by

$$\hat{\omega}(T) - \hat{\omega}_0 = \frac{2m^{1/2}}{\bar{\delta}}[Y(T) - Y_0], \tag{43}$$

$$\frac{1}{\hat{\omega}^2(T)} - \frac{1}{\hat{\omega}_0^2} = 4\left\{T - [Y(T) - Y_0]/\bar{\delta}\right\}, \tag{44}$$

where the index 0 denotes the initial value at $T = 0$. Since the quasi-particles (perturbations) enter into the plasma at the boundary, we set $Y_0 = 0$ in Eqs. (43) and (44). Combining Eqs. (43) and (44) we obtain the frequency $\hat{\omega}(T, Y)$ as a function of time and space, i.e.,

$$\frac{1}{\hat{\omega}^2} - \frac{1}{(\hat{\omega} - 2Ym^{1/2}/\bar{\delta})^2} = 4(T - Y/\bar{\delta}). \tag{45}$$

We are mainly interested at the dynamics of the instability at time $T \sim 1$. By analyzing Eq. (45) one can distinguish several unstable regions with $\hat{\omega} \gtrsim m^{1/6}$. This gives

$$Im\hat{\omega} = -m^{1/6}\frac{\sqrt{3}}{2}\left[\frac{Y/\bar{\delta}}{|T - Y/\bar{\delta}|}\right]^{1/3}, \quad \text{for} |T - Y/\bar{\delta}| \ll 1/m, \tag{46}$$

$$Im\hat{\omega} = -\frac{1}{\sqrt{4|T - Y/\bar{\delta}|}}, \text{for} |T - Y/\bar{\delta}| \gg 1/m, \quad Y/\bar{\delta} - T \lesssim m^{-1/3} \lesssim Y/\bar{\delta}. \tag{47}$$

The gain function $G(Y, T)$ is given by

$$G(x,t) = \int_{x/V_b^0}^{t} Im\omega(x,\bar{t})d\bar{t}, \tag{48}$$

For $T \sim 1$, the gain function $G(Y,T)$ is zero everywhere except in the region near the plasma entry, where $0 < Y < T\bar{\delta}$. Substituting Eqs. (46) and (47) into Eq. (48) one finds that the resonant region in Eq. (46) gives a contribution which is $m^{1/2}$ times smaller than the contribution from the region in Eq. (47). Up to this small factor, the gain function can be approximated by

$$G(Y,T) \approx \omega_{pi} T_f \sqrt{T - Y/\bar{\delta}} \tag{49}$$

for $Y < \bar{\delta}T$. Some portion of the beam will be present in this region close to the beam entrance up to the time

$$t_{max} = L_b^0/(V_b^0 + \Delta V_b^0) = T_f \frac{\Delta V_b^0/V_b^0}{1 + \Delta V_b^0/V_b^0}, \tag{50}$$

which corresponds to a value of the normalized time variable given by $T_{max} = \log(1 + \Delta V_b^0/V_b^0)$. For sufficiently small value of the velocity tilt, $T_{max} \approx \Delta V_b^0/V_b^0 \ll 1$, and the approximation $\bar{\delta}(T) = \bar{\delta}_0 \exp(T) \approx \bar{\delta}_0$ that was made in the derivation of Eq. (49) is justified. Therefore the maximum value of the gain function, which is reached near the beam entrance, is given by

$$G_{max} \approx \omega_{pi} T_f (\Delta V_b^0/V_b^0)^{1/2}. \tag{51}$$

6. Conclusions

The electrostatic two-stream instability for a cold, longitudinally-compressing ion beam propagating through a background plasma has been investigated analytically from the point of view of wave dynamics, where the plasma waves are represented as quasi-particles characterized by their position $x(t)$, wavenumber $k(t)$ and energy (or frequency) $\omega(t)$. For a low-density ion beam propagation in a background plasma with $\bar{\delta} \equiv Z_b n_b^0/n_0 \ll 1$ we identified two separate stages (the fast and the slow stages) of the two-stream instability. During the fast stage, the instability is between the neutralizing plasma electrons, flowing with the velocity $\sim (n_b/n_e)V_b$, and the background plasma ions. During this initial stage, the beam ions are relatively unaffected. We find that due to the small velocity of the neutralizing background electrons, the quasi-particles do not propagate far from the plasma boundary, and the instability is limited to the region $x < (n_b/n_e)X_f \ll X_f$. The rate of the instability growth and the number of e-folding are significantly affected by the velocity tilt [Eq. (51)]. At later times, a two-stream instability between the beam ions and the neutralizing background plasma electrons may develop. During this later stage of instability, which directly affects the beam ions, it is found that the longitudinal beam compression strongly modifies the space-time development of the instability. In particular, the dynamic compression leads to a significant reduction in the growth rate of the two-stream instability compared to the case without an initial velocity tilt by a factor $G_{max}/G_{max}^{notilt} \sim (\omega_{pb}/\omega_{pe})^{1/3} \ll 1$. The number of e-foldings is proportional to the number of beam-plasma periods $1/\omega_{pb}$ during the compression time T_f. The two-stream instability is complectly mitigated by the effects of dynamical beam compression when $\omega_{pb} T_f \lesssim 1$.

Acknowledgement

This research was supported by the U. S. Department of Energy.

[1] E. A. Startsev and R. C. Davidson, New Journal of Physics **6** (2004) 141.
[2] E. A. Startsev and R. C. Davidson, Phys. Plasmas **13** (2006) 062108.
[3] P. K. Roy, S. S. Yu, E. Henestroza *et al.*, Phys. Rev. Lett. **95** (2005) 234801.
[4] C. Thoma, D. R. Welch, S. S. Yu, E. Henestroza, P. K. Roy, S. Eylon, and E. P. Gilson, Phys. Plasmas **12** (2005) 043102.
[5] P. K. Roy S. S. Yu, S. Eylon *et al.*, Phys. Plasmas **11** (2004) 2890.
[6] D. R. Welch, D. V. Rose, T.C. Genoni, S. S. Yu and J. J. Barnard, Nucl. Instrum. Methods Phys. Res. A **544** (2005) 236.
[7] I. Kaganovich, E. A. Startsev and R. C. Davidson, Phys. Plasmas **11** (2004) 3546.
[8] R. Briggs, in: A. Symon and W. B. Thompson (Eds.), Advances in Plasma Physics, Interscience, New York, 1971, Vol. 4, p.43.
[9] R. C. Davidson, I. Kaganovich, H. Qin, E. A. Startsev, D. R. Welch, D. V. Rose, and H. S. Uhm, Phys. Rev. ST Accel. Beams **7** (2004) 114801.
[10] H. Qin, E. A. Startsev and R. C. Davidson, Phys. Rev. ST Accel. Beams **6** (2003) 014401.
[11] H. Qin, Physics of Plasmas **10** (2003) 2708.
[12] R. C. Davidson and H. Qin, Physics of Intense Charged Particle Beams in High Energy Accelerators, World Scientific, Singapore, 2001, and references therein.
[13] D. D. Ryutov, Sov. Phys.-JETP **30** (1970) 131.
[14] E. P. Lee, Simon Yu, H. L. Buchanan, F. W. Chambers and M. N. Rosenbluth, Phys. Fluids **23** (1980) 2095.
[15] T. C. Genoni, D. V. Rose, D. R. Welch and E. R. Lee, Phys. Plasmas **11** (2004) L73.
[16] P. Stroud, Laser and Particle Beams **4** (1986) 261.
[17] FEMLAB Reference Manual, Comsol AB, Stockholm, Sweden, version 2.2 ed. (2001).